


## Research

# CO<sub>2</sub>-free production of hydrogen via pyrolysis of natural gas: influence of non-methane hydrocarbons on product composition, methane conversion, hydrogen yield, and carbon capture

Ahmet Çelik<sup>1</sup>  · Iadh Ben Othman<sup>1</sup> · Heinz Müller<sup>1</sup> · Olaf Deutschmann<sup>1</sup>  · Patrick Lott<sup>1</sup> 

Received: 4 July 2024 / Accepted: 27 October 2024

Published online: 06 November 2024

© The Author(s) 2024 

## Abstract

Methane pyrolysis represents a CO<sub>2</sub>-free hydrogen production route that enables simultaneous carbon capture. While the majority of previous studies in the field focus on pure CH<sub>4</sub> as feed gas stream, commercial processes will typically rely on natural gas as feedstock that contains also non-methane hydrocarbons such as ethane, propane, and n-butane. Therefore, the present study evaluates how CH<sub>4</sub> conversion, H<sub>2</sub> selectivity, product composition, and solid carbon yield evolve when using either pure CH<sub>4</sub> or synthetic natural gas (SNG) as feed gas stream for a thermal pyrolysis process in a lab-scale high-temperature reactor. For this, industrially viable conditions are applied, namely temperatures between 1000 °C and 1600 °C, residence times between 1 s and 7 s, and molar H<sub>2</sub> dilution ratios between 1:1 and 4:1. Although the use of SNG results in slightly lower hydrocarbon conversions because the additional components in SNG result in a higher effective H<sub>2</sub> dilution ratio compared to a CH<sub>4</sub>-only feed, the non-methane hydrocarbons in the SNG have a positive effect on both H<sub>2</sub> selectivity and solid carbon yield. Taking existing mechanistic understanding into account, these positive effects are attributed to radicals formed from the non-methane hydrocarbons, which facilitate dehydrogenation steps from ethane to ethylene and hereby increase the relative amount of H<sub>2</sub> originating from CH<sub>4</sub>. The introduction of a carbonaceous fixed bed further benefits the performance of the pyrolysis process and ultimately enables to capture more than 98% of carbon in its solid form under industrially viable process conditions.

## 1 Introduction

On the way towards a novel and sustainable energy system, hydrogen (H<sub>2</sub>) is considered as one of the most important and promising carbon-free energy carriers [1–3]. In this regard, a wide variety of climate-friendly technologies that rely on H<sub>2</sub> enjoys growing popularity, for instance H<sub>2</sub>-fueled internal combustion engines in stationary power plants or heavy duty and off-road applications [4, 5], fuel cells [6, 7], and large-scale processes in metallurgy and steel industry [8–10]. However, to date steam reforming of fossil natural gas with its main component methane (CH<sub>4</sub>), which causes substantial carbon dioxide (CO<sub>2</sub>) emissions, accounts for the majority of the global H<sub>2</sub> production [11]. Since water electrolysis, which is the only entirely carbon-free H<sub>2</sub> production route, requires comparably high investment costs and suffers from technological hurdles, alternative routes are investigated.

✉ Patrick Lott, patrick.lott@kit.edu | <sup>1</sup>Institute for Chemical Technology and Polymer Chemistry (ITCP), Karlsruhe Institute of Technology (KIT), Engesserstr. 20, 76131 Karlsruhe, Germany.



Technical carbon (carbon black), which is used mainly as reinforcement material in rubber, represents another important feedstock for the industry with a large CO<sub>2</sub> footprint: In fact, the production route of this material, so-called furnace processes, are associated with emissions between approx. 1.9 and 5.2 kg CO<sub>2</sub> per kg carbon black [12].

In this regard, methane pyrolysis is considered by both academia and industry as a feasible technology for a sustainable production of hydrogen and carbon black [13, 14]. Herein, various demonstration plants have already been developed. Among these, the electrically heated moving bed process by BASF [15], which uses amorphous carbon to facilitate deposition reactions, and the process from Monolith Materials [16], which uses a plasma torch for heat provision, are particularly noteworthy. Both processes are designed to enable a commercialization of both carbon and hydrogen production. Therefore, methane pyrolysis would decarbonize two value chains, namely the hydrogen and carbon production routes.

With a significantly lower energy demand than water electrolysis and without any direct CO<sub>2</sub> emissions [17–23], CH<sub>4</sub> pyrolysis is referring to the endothermic thermal decomposition of methane according to Eq. (1), producing gaseous H<sub>2</sub> and solid carbon [24–27]:



Under standard conditions, the reaction enthalpy  $\Delta_r H^\circ$  is 75 kJ mol<sup>−1</sup>, which increases with increasing temperature, i.e. to 82 kJ mol<sup>−1</sup> at 1000 °C [27]. In brief, the underlying reaction mechanism consists of a large number of elementary reactions involving the coupling of CH<sub>4</sub> molecules to ethane (C<sub>2</sub>H<sub>6</sub>) and its dehydrogenation to ethylene (C<sub>2</sub>H<sub>4</sub>) and finally to acetylene (C<sub>2</sub>H<sub>2</sub>) [28, 29]. Subsequently, the coupling of C<sub>2</sub>H<sub>2</sub> yields benzene (C<sub>6</sub>H<sub>6</sub>) molecules, which then form polyaromatic hydrocarbons (PAH) that ultimately agglomerate to form solid carbon [30–34]. An entirely thermal decomposition of CH<sub>4</sub> requires temperatures above 1000 °C [35]. Although the catalytic decomposition of methane using iron- or nickel-based materials as catalysts, for example, allows for considerably high CH<sub>4</sub> conversions and H<sub>2</sub> selectivities already at temperatures between 500 °C and 1000 °C [36, 37], deactivation due to coking and metal impurities in the accruing carbon are major hurdles. As the commercialization of the solid product is essential for the profitability of the overall process [38, 39], a high purity and a high proportion of graphite in the solid product is desirable. Hence, thermal CH<sub>4</sub> pyrolysis does not only ensure longer operating times, but also makes a further and possibly energy-intensive treatment of the accruing carbon redundant [40]. Notably, carbon itself can act as a catalyst, because it provides additional surface area for autocatalytic particle growth via heterogeneous adsorption and decomposition reactions and hereby promotes CH<sub>4</sub> conversion [41–43].

For a more holistic view of the CH<sub>4</sub> pyrolysis process, a mass and energy balance is essential, as depicted in Eq. (2) and Eq. (3) [18].

$$\text{Mass : } 1 \text{ t CH}_4 \rightarrow 250 \text{ kg H}_2 + 750 \text{ kg C} \quad (2)$$

$$\text{Energy : } 50000 \text{ MJ} + \Delta_r H^\circ \rightarrow 30000 \text{ MJ} + 24600 \text{ MJ} \quad (3)$$

The mass balance (Eq. 2) shows that carbon is the main product of the pyrolysis process in terms of mass. It is therefore obvious that a further utilization of the accruing carbon is highly desirable in order to design an efficient overall process with high economic appeal. Furthermore, the energy balance (Eq. 3), which consists of the heating values of methane, hydrogen, and carbon (corresponding to the respective oxidation reaction), suggests a significant energy loss in the gas-phase, because also solid carbon “contains” a significant amount of energy. Hydrogen from pyrolysis may serve as clean fuel, which in contrast to direct methane combustion does not result in CO<sub>2</sub> emissions, or may be utilized in chemical industry. If CO<sub>2</sub> taxation is taken into consideration, a simple storage of accruing carbon may be economically feasible at some point in the future. However, in order to avoid wasting the energy stored in solid carbon, its utilization is reasonable. If the carbon is not only to be stored but also utilized (both alternatives are currently the subject of debate [13, 44, 45]), it must also be taken into account that the global carbon market, at an estimated 14–24 Mt [46], is significantly smaller than the demand for hydrogen (200–600 Mt) [47]. In this case, methane pyrolysis would primarily serve as a complementary technology that is adapted to the global demand for carbon. Notably, also novel areas of application are evaluated in order to utilize the vast amounts of solid carbon, e.g. soil amendment for agricultural areas or creation of new land in waterfront areas [45, 48], which could increase the global carbon demand significantly.

In terms of potential feedstocks, to date, fossil natural gas, which contains also nitrogen (N<sub>2</sub>), short-chain hydrocarbons such as C<sub>2</sub>H<sub>6</sub>, propane (C<sub>3</sub>H<sub>8</sub>), or n-butane (C<sub>4</sub>H<sub>10</sub>), and CO<sub>2</sub> [49] represents the main source of CH<sub>4</sub>. Therefore, the direct usage of natural gas during the pyrolysis process appears particularly convenient. In this context, the thermal decomposition of several hydrocarbons as well as natural gas was studied in the past [50–52]. Since some of those hydrocarbons

also act as precursors during carbon formation, the influence of these precursors on product composition,  $\text{CH}_4$  conversion, and especially  $\text{H}_2$  selectivity in a process with  $\text{CH}_4$  as main component in the feed is of particular interest in order to design a suitable pyrolysis reactor. Herein, experimental studies on natural gas mixtures for methane pyrolysis exist in the literature [29, 53–55]. Although the influence of ethane, propane or DME as additional hydrocarbons were examined [56], these studies employed comparatively short residence times ( $< 10^{-2}$  s), frequently aiming to achieve a high yield of coupling products. However, the formation of the latter should be avoided in a pyrolysis process, where higher residence times ( $> 1$  s) are required for sufficient hydrogen and carbon yields [40]. Moreover, political tensions in the energy market and fluctuating resources call for a flexible operation of industrial  $\text{CH}_4$  pyrolysis processes that can cope with variable feed gas streams [57]. Hence, the differences between both feed streams—i.e. pure  $\text{CH}_4$ , e.g. from purified renewable biogas [58], and conventional natural gas—must be clarified with a re-arranged focus on decomposition products in order to ensure the establishment of a cost-efficient and reliable large-scale and  $\text{CO}_2$ -free  $\text{H}_2$  production route.

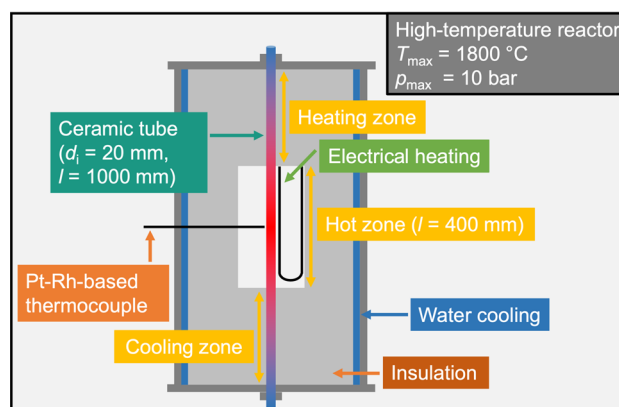
Consequently, the current study investigates the thermal pyrolysis of both, natural gas and pure  $\text{CH}_4$ , and aims at optimizing the operating parameters in terms of  $\text{CH}_4$  conversion,  $\text{H}_2$  selectivity, product composition, as well as solid carbon yield. For this, the influence of temperature, residence time, and  $\text{H}_2$  dilution is studied in detail, in particular taking the impact of the additional species in natural gas on the pyrolysis into account. In addition to empty tube experiments, reactor operation with a carbonaceous fixed bed is evaluated in order to obtain extensive knowledge with regard to more realistic reactor configurations that promote  $\text{CH}_4$  conversion and the selectivity to the desired product  $\text{H}_2$  and that are of industrial relevance.

## 2 Methods

The experiments for this study were conducted in an in-house developed setup that was designed for experiments at high temperature and elevated pressure and which was already introduced in previous publications of our group [40, 58, 59]. It essentially consists of a gas dosing system that feeds the reaction gases (provided by gas bottles) via mass flow controllers (Bronkhorst), a tubular  $\alpha\text{-Al}_2\text{O}_3$  reactor (length = 100 cm, diameter = 2 cm; DEGUSSIT AL23 by Friatec/Aliaxis) that can be heated to 1800 °C by heating elements and that is placed in an insulated stainless-steel vessel (schematic drawing given in Fig. 1), and an analysis section. The effluent product gas stream was continuously analyzed with a mass spectrometer (Hiden Analytical HPR 20 R&D). While a trap downstream of the reactor allowed the separation of the majority of solid particles, an additional particle filter prior to the analysis section removed also fine soot particles. Experiments were performed either with an empty reactor tube, or the reactor was filled with a carbonaceous fixed bed consisting of acetylene coke pellets (Carbolux, supplied by BASF SE) with an average pellet diameter of 2 mm to 3 mm.

As already described in detail in a previous publication [58], these pellets were filled into a container made of graphite foil (190 mm height), which was mounted in the reactor in such a way that the distance between the upper end of the fixed bed (height = 75 mm) and the reactor inlet was 380 mm. This ensured that the feed gases were heated to the appropriate reaction temperature before reaching the fixed bed. In this regard, either pure methane or synthetic natural gas (SNG, AirLiquide, consisting of  $\text{CH}_4$  with 81.2684 vol.-%,  $\text{C}_2\text{H}_6$  with 2.9710 vol.-%,  $\text{C}_3\text{H}_8$  with 0.4913 vol.-%,  $\text{C}_4\text{H}_{10}$  with 0.0993 vol.-%,  $\text{N}_2$  with 14.1600 vol.-%,  $\text{CO}_2$  with 1.0100 vol.-%) was used as feed gas in this work.

**Fig. 1** Schematic drawing of the reactor setup with descriptive captions



In addition to temperature, also pressure represents an important process parameter. While high pressure is thermodynamically not favorable for the methane conversion, a moderate pressure increase can inhibit the formation of byproducts such as  $C_2$  and  $C_3$  species or benzene [60]. In order to avoid the potential overlap of feed gas-related phenomena with pressure-induced effects, all experiments were carried out at atmospheric pressure. This approach enables to gain an unbiased understanding on the formation and possible influence of intermediates and SNG components.

In this respect, also the dilution of the reaction gases with  $H_2$  throughout all experiments presented herein counteracts clogging in the reactor due to the formation of solid carbon and thus helps to avoid an undesired pressure increase during reactor operation that would impede drawing solid conclusions on the gas-phase chemistry. Exploiting  $H_2$ , which is an integral part of the product gas stream anyways, as diluent is particularly relevant also in the context of a potential industrially viable natural gas pyrolysis process, because it eliminates the need for downstream product separation. This outweighs the inhibition of the pyrolysis reaction by  $H_2$  that has been reported in the past [60, 61], especially considering that this inhibition is only comparably moderate at industrially viable high temperatures. Therefore,  $H_2$  was chosen as dilution gas for the present study. After the diluted reaction gases were fed into the reaction tube for 20 min at reaction temperature, the reactor was purged with argon (Ar). Subsequently, for experiments in an empty reactor tube, any deposits that may have formed during the experiment were burned off with synthetic air. In fixed-bed experiments, on the other hand, the reactor was cooled down to ambient temperature while purging with inert gas and graphite container with the fixed bed was removed.

During data evaluation, the volume fraction of each species in the product stream was measured in steady-state via mass spectrometry. Herein, the MS data was averaged over the entire steady-state, whereby the mean deviation of the MS data was less than 2%. Consecutively, the molar flow rate of each gas-phase species was calculated by using H balance for the total flow rate (considering gas expansion) and multiplying it with the respective mole fraction. Based on the gas-phase data, key descriptors such as hydrocarbon conversion (X),  $H_2$  selectivity (S), and solid carbon yield (Y) were calculated according to Eqs. (4–9): Eqs. (4, 6, and 8) were used for a  $CH_4$ -only feed, whereas Eqs. (5, 7, and 9) were used for SNG as feed. Herein,  $\dot{N}$  describes the molar flow and  $\nu$  is the stoichiometric factor for  $H_2$  from the respective hydrocarbon (e.g., 3 for ethane or 4 for propane). Note, that for SNG as feed the conversion of all hydrocarbons (HC) in the reactant stream was considered for conversion,  $H_2$  selectivity, and solid carbon yield.

$$X_{CH_4} = \frac{\dot{N}_{CH_4}^{in} - \dot{N}_{CH_4}^{out}}{\dot{N}_{CH_4}^{in}} \cdot 100\% \quad (4)$$

$$X_{HC} = \frac{\sum_i (\dot{N}_{HC_i}^{in} - \dot{N}_{HC_i}^{out})}{\sum_i \dot{N}_{HC_i}^{in}} \cdot 100\% \quad (5)$$

$$S_{H_2, CH_4} = \frac{\dot{N}_{H_2}^{out} - \dot{N}_{H_2}^{in}}{2(\dot{N}_{CH_4}^{in} - \dot{N}_{CH_4}^{out})} \cdot 100\% \quad (6)$$

$$S_{H_2, HC} = \frac{\dot{N}_{H_2}^{out} - \dot{N}_{H_2}^{in}}{\sum_i \nu_i (\dot{N}_{HC_i}^{in} - \dot{N}_{HC_i}^{out})} \cdot 100\% \quad (7)$$

$$Y_{C, CH_4} = \frac{\dot{N}_C^{out}}{\dot{N}_{CH_4}^{in}} \cdot 100\% \quad (8)$$

$$Y_{C, HC} = \frac{\dot{N}_C^{out}}{\sum_i \nu_i \dot{N}_{HC_i}^{in}} \cdot 100\% \quad (9)$$

### 3 Results and discussion

In a first step, the high-temperature setup described in the previous section was used to systematically investigate the influence of temperature (1000 °C, 1200 °C, 1400 °C, and 1600 °C), residence time (1 s, 3 s, 5 s, and 7 s), and molar  $H_2$  dilution ratio of the feed gas containing either pure  $CH_4$  or SNG on hydrocarbon conversion,  $H_2$  selectivity, product composition as well as solid carbon yield. Particular focus is laid on the impact of SNG-components. Note that if SNG is used as feed, the molar  $H_2$  dilution ratio refers to all SNG components, including  $N_2$ ; consequently, an overall higher  $H_2$ :hydrocarbon ratio is present during experiments with SNG feeds. In addition to gas-phase experiments, the impact of a carbonaceous fixed bed in the reactor is studied.

#### 3.1 Role of non-methane hydrocarbons at varying reaction conditions

In order to investigate the effect of temperature on the reaction process, the pyrolysis of pure  $CH_4$  and of SNG is studied at a molar  $H_2$  dilution ratio of 2:1 and a residence time of 5 s while varying the temperature from 1000 °C to 1600 °C. Figure 2 summarizes the data obtained during gas-phase tests in an empty reactor configuration, namely the molar hydrocarbon conversion (Fig. 2a), molar  $H_2$  selectivity (Fig. 2b), and product composition (Fig. 2c) for both feed compositions, pure  $CH_4$  and SNG (both diluted with  $H_2$ ) as a function of the reaction temperature.

As shown in Fig. 2a, hydrocarbon conversion increases from about 20% and 30% for  $CH_4$  and SNG, respectively, at 1000 °C to more than 80% at 1400 °C and to almost full conversion at 1600 °C, irrespective of the feed. Note that for the sake of comparability, not only methane but also the conversion of ethane, propane and n-butane was included in the calculation if SNG served as a feed (c.f. Eq. (5)). Taking the overall hydrocarbon conversion into account, it becomes apparent that the hydrocarbon conversion for SNG is always slightly lower than the values for pure methane as feed for the entire temperature range investigated herein. This can be explained by the  $H_2$  dilution, which is defined as the molar ratio between hydrogen and either methane or SNG in the feed stream. Since SNG contains over 14%  $N_2$ , the effective ratio between  $H_2$  and the hydrocarbons that can be pyrolyzed is higher than for a feed gas with pure  $CH_4$ . The higher number of hydrogen molecules inhibits each dehydrogenation step, which not only comprises the initial pyrolysis reaction step of methyl radical formation, but also the dehydrogenation of ethane to ethylene and acetylene, respectively [26, 62]. In

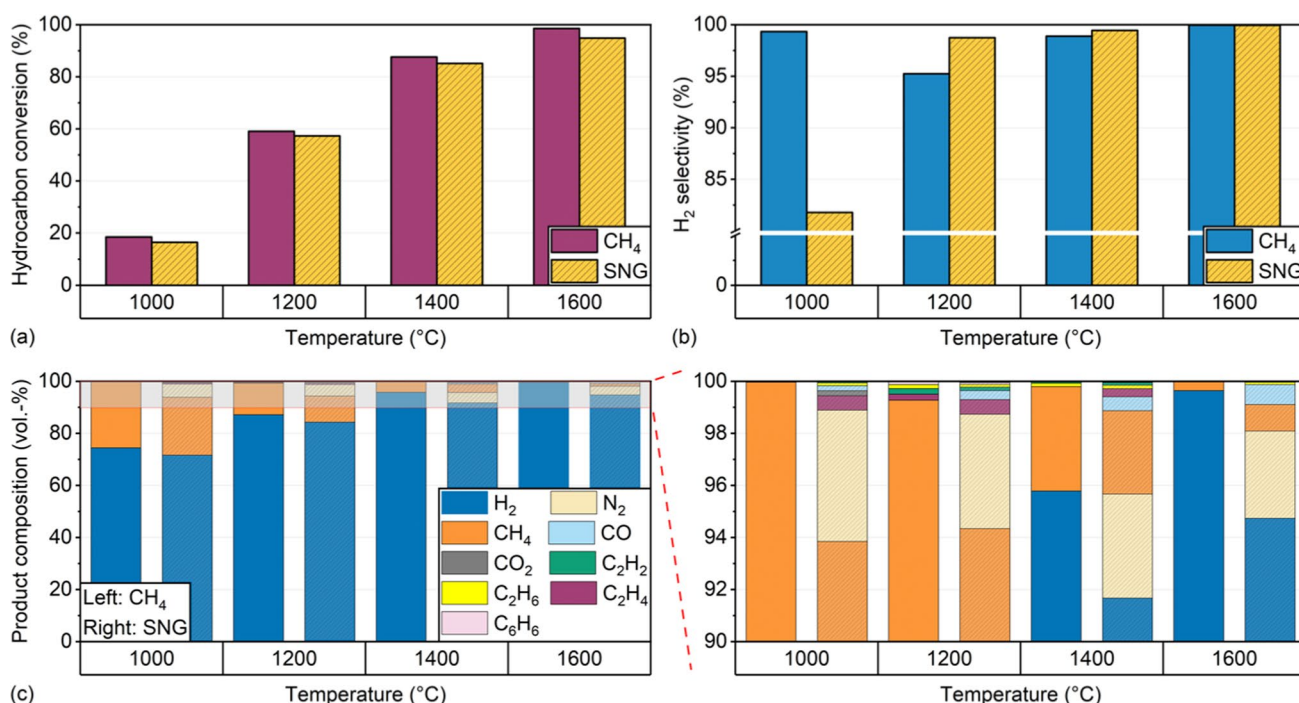


**Fig. 2** Molar hydrocarbon conversion (a), molar  $H_2$  selectivity (b), and product composition (c) for pure  $CH_4$  and SNG as feed at temperatures from 1000 °C to 1600 °C, a residence time of 5 s, and molar  $H_2$  dilution ratio ( $H_2$ : $CH_4$  and  $H_2$ :SNG) of 2:1



this context, the additional hydrocarbons contained in the SNG might affect the hydrocarbon conversion as well: While the presence of  $C_2$  species might shift the equilibrium towards methane and the presence of propane might increase hydrocarbon conversion, the higher effective  $H_2$ :hydrocarbon ratio is assumed to be the dominating factor governing the hydrocarbon conversion during experiments conducted with an SNG feed.

According to the data presented in Fig. 2b, the  $H_2$  selectivity trends depend on the feed gas. For a  $CH_4$ -only feed, the temperature has only a minor influence on the  $H_2$  selectivity, which always exceeds 95%. A local minimum in  $H_2$  selectivity is observed at 1200 °C, which correlates with the higher levels of byproducts that were observed at this temperature (Fig. 2c). If SNG is used as feed instead, the  $H_2$  selectivity is initially below 80% at 1000 °C. At a temperature of 1200 °C and above it always exceeds 97%, which is higher than the corresponding values for a  $CH_4$ -only feed.

The product composition (Fig. 2c) shows that for a  $CH_4$ -only feed, ethane, ethylene, acetylene as well as benzene were mainly found at 1200 °C and 1400 °C, with a total byproduct concentration of less than 1%. The local maximum in byproduct concentrations at 1200 °C corresponds to the local  $H_2$  selectivity minimum. Since all byproducts observed herein are known to act as intermediates during the  $CH_4$  pyrolysis reaction, we can conclude that an incomplete  $CH_4$  decomposition reaction and possible reverse reactions account for this selectivity minimum, which is in line with previous findings [40, 58, 61]. As the  $CH_4$  conversion increases upon a further temperature increase, the volumetric  $CH_4$  content drops below 1% at 1600 °C and the formation of byproducts becomes negligible, which confirms earlier findings from our group [40, 58]. Analogous to the measurements with a  $CH_4$ -only feed, ethane, ethylene, acetylene and benzene are identified as additional byproducts also for an SNG feed gas stream, however, their concentration is generally higher. Once again, concentration maxima of the above-mentioned short-chain hydrocarbons and of benzene are found at 1200 °C, which corresponds to the slightly lower  $H_2$  selectivity, and byproducts become almost negligible at 1600 °C. For experiments with SNG feeds, particularly the concentration of ethylene is higher compared to experiments conducted with pure  $CH_4$  as feed and exhibits a maximum of more than 0.5% at 1200 °C (Fig. 2c).

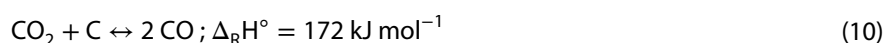
To comprehensively explain these results, the byproduct formation pathways need to be discussed in more detail. Gaining a deeper understanding on the reaction pathways of the non-methane hydrocarbons in the SNG can be gained especially at low temperatures, because the reactivity of the most stable  $CH_4$  molecule is lower than that of any other hydrocarbon [61], which typically decompose at lower temperatures than  $CH_4$  [63]. With increasing temperature, the contribution of  $CH_4$  to the total hydrocarbon conversion becomes dominant and hereby impedes the identification of reaction pathways. Consequently, a temperature-induced acceleration of the pyrolysis reactions leads to an initially increased formation of gaseous intermediates before essentially all intermediates are consumed during solid carbon formation at very high reaction temperatures. Note, that the temperature profile inside the high-temperature reactor used for the present study includes a heating zone, an isothermal reaction zone (hot zone), and a cooling zone (Fig. 1), as already reported in a previous publication [64]. Herein, it can be assumed that the pyrolysis of higher hydrocarbons such as the  $C_2$  and  $C_3$  species in the SNG already starts in the heating zone and thus at lower temperatures compared to the decomposition of methane. Such a “pre-pyrolysis” may promote the overall hydrocarbon conversion, which could also be exploited in technical full-scale processes.

The comparably low  $H_2$  selectivity for the SNG feed gas stream at 1000 °C (Fig. 2b) is primarily a consequence of the high  $C_2H_4$  mole fraction of approximately 0.5% (Fig. 2c). While methane conversion at this temperature is only 13.3%, the overall hydrocarbon conversion (including  $C_2H_6$ ,  $C_3H_8$ , and  $C_4H_{10}$  as well) is 16.5%. In contrast,  $CH_4$  is the only hydrocarbon in the effluent product gas stream if a  $CH_4$ -only feed is used and the corresponding conversion is found to be 20%. Under consideration of the hydrocarbon levels in the feed gas and after comparison with the results for the  $CH_4$ -only feed, we conclude that a significant amount of the formed  $C_2H_4$  originates from the additional hydrocarbons. In particular, we assume that the higher  $C_2H_4$  levels result from incomplete dehydrogenation of  $C_2H_6$ , which is a key step in the reaction mechanism of hydrocarbon pyrolysis [29]. In fact, all the molecules found as byproducts act as intermediate species during the formation of PAHs and subsequent soot and solid carbon formation [40, 65]. By using an SNG feed instead of a  $CH_4$ -only feed gas, byproducts from methane pyrolysis and thus essentially intermediate species are added to the reaction gas mixture right from the beginning, which benefits  $CH_4$  pyrolysis. In particular, the decomposition of the ethane molecule results in the formation of methyl radicals, which can accelerate dehydrogenation reactions in general, especially the formation of further methyl radicals from  $CH_4$  molecules [66] that is considered to be the rate-limiting step of the overall methane pyrolysis reaction [67, 68]. Data presented below will further support this assumption.

It has also been reported that  $CH_3^{\cdot}$  and  $C_2H_3^{\cdot}$  radicals can form propylene and toluene, which do not follow the conventional reaction route to polyaromatic hydrocarbons via benzene and acetylene [66]. Therefore, their formation would reduce both the production of elemental hydrogen in the gas-phase as well as the carbon fixation in the solid product. However, neither propylene nor toluene were detected in the product gas stream, irrespective of the reaction

parameters, which is most likely due to the significant higher reaction temperature compared with the data from literature [66], as such high temperatures favor the reaction towards ethane and a consecutive dehydrogenation towards acetylene instead of propylene formation.

Furthermore, if SNG is used as feed, the volumetric share of  $N_2$  in the effluent gas stream decreases from 4.5% at 1000 °C to 3% at 1600 °C (Fig. 2c), despite  $N_2$  can be considered fairly inert under the conditions applied herein. As neither the N-balance nor a qualitative screening of possible N-containing mass fragments by mass spectrometry suggest a relevant conversion of  $N_2$ , we attribute the declining  $N_2$  concentration to the increasing  $CH_4$  conversion, which results in an increased product volume flow rate (c.f. Eq. (1)). This is further underscored when the  $N_2$  mass flow upstream and downstream of each experiment is compared: the relative deviation is less than 0.15% and thus well below the experimental error bars of the mass spectrometer data. Since SNG contains approx. 1%  $CO_2$ , the product gas stream contains  $CO_2$  and also CO. While at 1000 °C approx. 40% of  $CO_2$  are converted to CO, which corresponds to an absolute CO concentration of less than 0.2% in the product gas stream, higher temperatures ensure complete  $CO_2$  conversion, culminating in about 0.7% CO at 1600 °C. This observation can be explained with the Boudouard equilibrium (shown in Eq. (10)), which has been reported as a relevant reaction under pyrolytic conditions [58] and which shifts to the side of CO with increasing temperature [27, 69].



Since the presence of  $CO_2$  or CO does not significantly influence the kinetics of pyrolysis, their separation can in principle take place both upstream and downstream. In the case of upstream purification of natural gas, the most common processes are amine scrubbing for the separation of CO/ $CO_2$  from natural gas [70] and glycol dehydration for the separation of water (another potential component of natural gas) [71]. Both approaches are based on an absorption process (in the case of CO/ $CO_2$  mostly in monoethanolamine and in the case of water mostly in triethylene glycol) and are well established. In the case of downstream purification of the product stream, pressure swing adsorption (PSA) with a suitable adsorbent is the common process for the separation of CO,  $CO_2$ , as well as water, which can provide hydrogen in very high degrees of purity, e.g. as commonly necessary for fuel cell applications [72, 73]. Since a downstream PSA is often required in an  $H_2$  production process anyway, e.g. in order to remove unreacted hydrocarbons from the product gas stream, a simultaneous downstream purification of CO and  $CO_2$  (and/or water, if applicable) could be the most elegant solution. However, as this will most likely depend on the process specifications and constraints of the production site, a generally valid statement cannot be given.

In addition to temperature, also residence time and  $H_2$  dilution play a decisive role during the pyrolytic decomposition of methane. Therefore, Fig. 3 shows  $CH_4$  conversion (a) and  $H_2$  selectivity (b) for both, a pure  $CH_4$  and SNG feed gas, as a function of residence time and molar  $H_2$  dilution ratio at 1200 °C and 1400 °C.

Although irrespective of the feed gas both  $CH_4$  conversion and  $H_2$  selectivity increase significantly with rising residence time at both 1200 °C and 1400 °C, the impact of residence time is higher at 1200 °C; due to a stronger kinetic promotion with increasing temperature, it becomes less pronounced at 1400 °C. Similarly, a higher  $H_2$  dilution, which is known to inhibit  $CH_4$  conversion and  $H_2$  selectivity [26], has a lower impact at 1400 °C than at 1200 °C. The inhibition itself can be explained by a direct influence of  $H_2$  on the kinetics as described above. Ultimately, this results in a lower  $CH_4$  conversion and a lower  $H_2$  selectivity [29, 62]. Among the conditions tested herein, a temperature of 1400 °C, a residence time

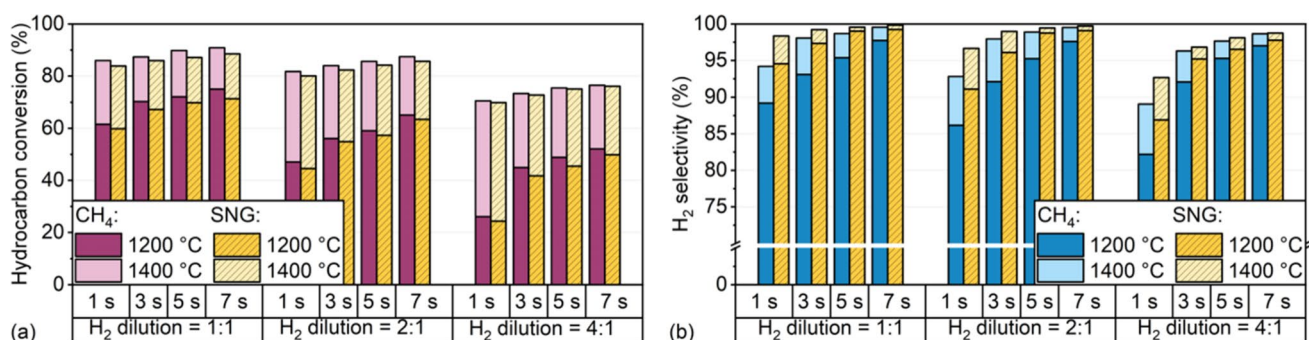


**Fig. 3** Molar hydrocarbon conversion (a) and molar  $H_2$  selectivity (b) for pure  $CH_4$  and SNG as a function of residence time and molar  $H_2$  dilution ratio ( $H_2:CH_4$  and  $H_2:SNG$ ) at 1200 °C and 1400 °C

of 7 s, and a H<sub>2</sub> dilution of 1:1 allow for the highest CH<sub>4</sub> conversion (almost 90%) and H<sub>2</sub> selectivity (> 99%) for both feed gas compositions.

Although in the investigated range of parameters the CH<sub>4</sub> conversion for both feeds gas compositions is in the same order of magnitude and shows similar trends, i.e. inhibition by H<sub>2</sub> and promotion by increased residence time, CH<sub>4</sub> conversions are at least slightly lower for experiments with SNG feeds. As already discussed above, this can be explained by a higher effective H<sub>2</sub> dilution if SNG is used as a feed, which contains about 14% N<sub>2</sub> and only approx. 81% CH<sub>4</sub>. Therefore, the SNG feed has a higher effective H<sub>2</sub>:CH<sub>4</sub> ratio than the CH<sub>4</sub>-only feed (both diluted in H<sub>2</sub>). In contrast, H<sub>2</sub> selectivities with SNG as feed are in general higher than with pure CH<sub>4</sub> as feed, which as mentioned before is most likely due to the presence of other hydrocarbons in SNG that are easier to convert. Their positive effect on H<sub>2</sub> selectivity is particularly relevant at low temperatures and short residence times. For instance, at a temperature of 1200 °C, a residence time of 1 s, and a H<sub>2</sub> dilution ratio of 1:1, the H<sub>2</sub> selectivity is 5.4% higher for experiments with SNG feed than for those with CH<sub>4</sub>-only feed. In contrast, the difference is only 0.3% at a temperature of 1400 °C, a residence time of 7 s, and a H<sub>2</sub>:SNG ratio of 1:1.

The higher H<sub>2</sub> selectivity for SNG cannot be explained by a simple additional formation of H<sub>2</sub> from the other hydrocarbons, as the selectivity value is a relative quantity. In particular, all H<sub>2</sub> selectivities plotted in the figures represent the net amount of elemental H<sub>2</sub> produced relative to the total amount of all hydrocarbons fed. In contrast, it can rather be assumed that the presence of the additional hydrocarbons favors the formation of H<sub>2</sub> from CH<sub>4</sub>, as already suggested above. In this context, it is worth taking a closer look at the amount of hydrogen produced. A maximum of 10.6% of the net H<sub>2</sub> produced (at a temperature of 1200 °C, a residence time of 1 s, and a molar H<sub>2</sub> dilution of 1:1) originates from the additional hydrocarbons in the SNG; the majority of the H<sub>2</sub> produced still comes from CH<sub>4</sub> (with a share that always exceeds 89.4%). In order to enable a quantitative statement, the H<sub>2</sub> selectivity for a CH<sub>4</sub>-only feed (Eq. 6) can be compared with an H<sub>2</sub> selectivity for the SNG feed gas, which only considers net produced H<sub>2</sub> originating from CH<sub>4</sub> (Eq. 11).

$$S_{\text{H}_2, \text{CH}_4} = \frac{(\dot{N}_{\text{H}_2}^{\text{out}} - \dot{N}_{\text{H}_2}^{\text{in}}) - \sum \nu_i (\dot{N}_{\text{HC}_i}^{\text{in}} - \dot{N}_{\text{HC}_i}^{\text{out}})}{2(\dot{N}_{\text{CH}_4}^{\text{in}} - \dot{N}_{\text{CH}_4}^{\text{out}})} \cdot 100\% \quad (11)$$

The formula shown in Eq. (11) sets the net amount of H<sub>2</sub> produced minus the amount of H<sub>2</sub> that originates from the additional hydrocarbons (assuming that all of those hydrocarbons are converted to elemental H<sub>2</sub> for the sake of simplification) in relation to the converted amount of methane. Thus, only the H<sub>2</sub> originating from CH<sub>4</sub> is taken into account (analogous to a CH<sub>4</sub>-only feed). Since the effect of additional hydrocarbon presence is most pronounced at 1200 °C, a residence time of 1 s, and a molar H<sub>2</sub> dilution of 1:1, these conditions are chosen for a direct comparison of the H<sub>2</sub> selectivity. While the H<sub>2</sub> selectivity calculated from Eq. (11) is 93.9% for SNG, the corresponding value for a CH<sub>4</sub>-only feed calculated according to Eq. (6) is only 89.2%. This means that the presence of non-methane hydrocarbons in SNG favors the relative amount of H<sub>2</sub> formed from CH<sub>4</sub> and obviously influences the reaction of CH<sub>4</sub> itself. Note, that while this effect is most pronounced at the above-mentioned set of reaction parameters, it can be observed for all considered parameters throughout this work. These findings do not only support previous studies that proposed a promoting effect of non-methane hydrocarbons on methane decomposition [50, 74], but are also in line with studies reporting that hydrocarbons such as ethane, propane, and butane begin to decompose at shorter residence times compared to methane [63, 66].

It is possible that either the formation of methyl radicals or the dehydrogenation of ethane and ethylene—all elementary steps during which hydrogen is released and thus which contribute to higher H<sub>2</sub> selectivity—is supported by previously formed radicals originating from the additional hydrocarbons, such as C<sub>2</sub>H<sub>3</sub><sup>·</sup>. An acceleration of the formation of CH<sub>3</sub><sup>·</sup> radicals would result in an increased CH<sub>4</sub> conversion for SNG as feed. However, the total hydrocarbon conversion as well as the pure CH<sub>4</sub> conversion is lower for SNG than for a CH<sub>4</sub>-only feed. Although the slightly higher H<sub>2</sub> dilution is a factor that could superimpose this effect (in the case of an H<sub>2</sub>:SNG dilution of 1:1 the effective H<sub>2</sub>:CH<sub>4</sub> dilution is as high as 1.2:1 for a SNG feed due to the N<sub>2</sub> content of about 14%), Fig. 3b clearly shows that an increase of the dilution from 1:1 to 2:1 does not have a particularly high impact on CH<sub>4</sub> conversion. We therefore assume that a favored methyl radical formation would result in a higher CH<sub>4</sub> conversion even with a slightly higher dilution ratio. Following this interpretation, the presence of non-methane hydrocarbons accelerates the dehydrogenation reactions, which explains both the higher H<sub>2</sub> selectivities as well as the very similar conversions obtained during experiments with SNG and CH<sub>4</sub>-only feeds. Notably, the temperatures in our experiments are significantly higher than in previous work that postulates the promotion of methyl radical formation [50, 63, 66, 74]. Due to these higher temperatures applied in the present work, the rate-determining character of this radical formation is expected to be less pronounced, which means that the acceleration through the addition of further intermediates is less pronounced as well.



**Fig. 4** Mass-based solid carbon yield as a function of residence time and  $H_2$  dilution at 1200 °C and 1400 °C for both SNG and pure  $CH_4$  as feed

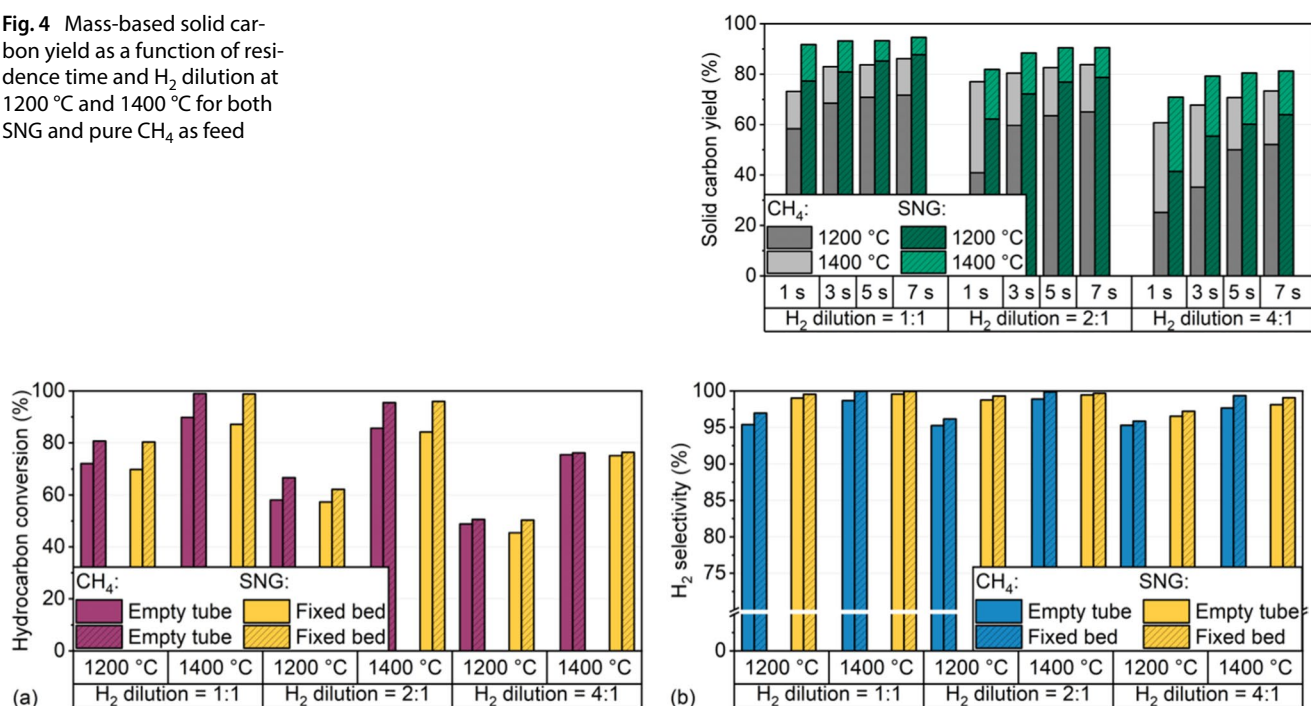


**Fig. 5** Empty tube and fixed bed results on molar hydrocarbon conversion (a) and  $H_2$  selectivity (b) for pure  $CH_4$  and SNG as a function of temperature and  $H_2$  dilution ratio at a constant residence time of 5 s

In order to evaluate the potential of the pyrolysis process to serve as a carbon sink, the amount of produced solid carbon in relation to the carbon entry in the form of  $CH_4$  and—if applicable—further carbon-containing molecules is calculated. In this regard, especially the potential positive influence of the additional non-methane hydrocarbons in the SNG on the solid formation is of interest. Figure 4 shows the mass-based solid carbon yield as a function of residence time and  $H_2$  dilution ratio at 1200 °C and 1400 °C for both  $CH_4$  and SNG as feed. The amount of carbon was calculated using a carbon balance that includes all C-containing gas-phase species detected end-of-pipe with the mass spectrometer. In addition to the uncertainty in quantifying the gas-phase species by means of mass spectrometry, PAHs that can accumulate in small amounts on solid carbon particles [65] and which are not analyzed quantitatively contribute to the error bar. Generously estimated we assume an error bar of about 5% for experiments with pure  $CH_4$  and approximately 7% for experiments with SNG, since the latter include more C-containing gas species with individual uncertainties in quantification.

The data shown in Fig. 4 suggest that the solid carbon yield increases with rising residence time and temperature and decreases with increasing  $H_2$  dilution, herewith directly corresponding to the methane conversion and  $H_2$  selectivity data shown in Fig. 3. The highest solid carbon yield of approx. 86% and 95% for a  $CH_4$ -only and a SNG feed, respectively, is found during reactor operation at 1400 °C with a  $H_2$  dilution of 1:1 and a residence time of 7 s. Hence, our results clearly underscore that not only  $CH_4$  but also the non-methane hydrocarbons in the SNG participate in the pyrolysis reactions, which is in line with the results on the (by-)product gas composition (c.f. Fig. 2c) and supports earlier findings [50, 66, 74]. For a potential real-world process, our present results imply that a purification of natural gas, apart from removing corrosive species such as sulfur oxides (S-levels of up to 5% have been found in natural gas [49]) that may accelerate degradation of reactor and setup parts, is not necessary. In fact, hydrocarbons such as ethane, propane, and butane were found to increase the  $H_2$  selectivity during our measurement campaign and may thus be even highly desirable in the feed gas stream.

### 3.2 Impact of a carbonaceous fixed bed

From previous research it is well known that carbon can act as a heterogeneous catalyst during pyrolysis reactions, as it provides active sites for the adsorption and dissociation of methane molecules, hereby facilitating the formation of radicals that play a crucial role in breaking the C-H bonds [40, 75, 76]. In this context, Fig. 5 compares  $CH_4$  conversion

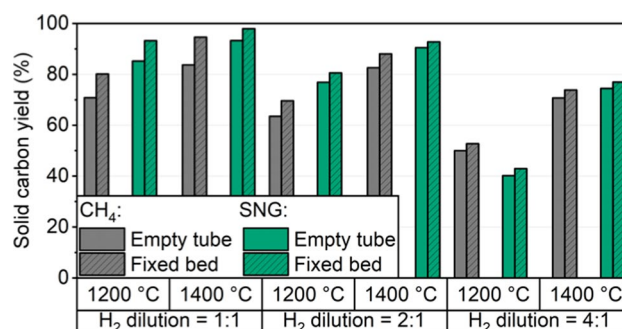
(a) and  $H_2$  selectivity (b) data obtained in an empty tube reactor configuration and from experiments during which the reactor was loaded with a carbonaceous fixed bed. While the residence time of 5 s was kept constant throughout all experiments (5 s were found to be sufficient for comparably high conversions [40, 58], with only minor changes if higher residence times were chosen), the temperature (1200 °C and 1400 °C), the  $H_2$ -feed gas ratio (1:1, 2:1, 4:1), and the feed gas itself ( $CH_4$ -only or SNG) were varied.

In general, a carbonaceous fixed bed was found to promote the conversion for both feeds, with a maximum conversion of almost 99% for pyrolysis of SNG at 1400 °C and a  $H_2$  dilution ratio of 1:1 (Fig. 5a). A qualitatively similar trend can be observed for  $H_2$  selectivity, even though with a less pronounced effect of the fixed bed, but with selectivities of up to almost 100% for SNG at 1400 °C and a  $H_2$  dilution ratio of 1:1 (Fig. 5b). These results confirm earlier studies [40, 43, 77] that uncovered the beneficial effect of carbon on the methane pyrolysis process. Notably, our results with SNG as feed suggest that additional hydrocarbons such as ethane, propane, and n-butane that are commonly present as minor components if SNG is used as feed gas may even enhance the positive influence of the carbon bed. Since these hydrocarbons act as intermediates during solid carbon formation from methane [26] and their decomposition is therefore easier than that of  $CH_4$  [63, 66], the deposition of newly formed carbon on the carbon particles of the fixed bed may be accelerated compared to experiments with a  $CH_4$ -only feed. This hypothesis also explains that the presence of a fixed bed diminishes the differences in conversion between experiments with a  $CH_4$ -only and SNG feed gas stream that was observed in an empty tube configuration. The data on the solid carbon yield depicted in Fig. 6, which correspond to the gas species data in Fig. 5, substantiates this assumption.

In general, higher temperatures, lower  $H_2$  contents, and the presence of a carbonaceous fixed bed benefit the carbon yield. At all temperatures and  $H_2$  dilutions tested herein, the fixed bed increases the yield of solid carbon, irrespective of the feed gas. Yields well above 70% can be achieved even for comparably high  $H_2$  dilution values of 4:1. In accordance with the conversion data depicted in Fig. 5a, the highest carbon yields are achieved at a temperature of 1400 °C and an  $H_2$  dilution of 1:1. Not only during empty tube experiments, but also during experiments with a fixed bed higher yields of solid carbon are found if SNG is used as feed gas, allowing a maximum carbon yield of almost 100% (1400 °C,  $H_2$  dilution of 1:1). Analogous to the previous discussion, we attribute the higher carbon yield for SNG feeds to the faster decomposition of the non-methane hydrocarbons  $C_2H_6$ ,  $C_3H_8$ , and  $C_4H_{10}$  compared to  $CH_4$  that is much more difficult to activate [63, 66]. Ultimately, this facilitates decomposition reactions because carbon that deposits on the fixed bed consisting of acetylene coke and on the reactor walls offers additional surface sites that catalyze heterogeneous decomposition reactions.

In this regard, amorphous carbon has been reported to exhibit a higher activity for methane decomposition than ordered carbons, which was attributed to structural defects acting as active sites for  $CH_4$  adsorption and dissociation reactions [75, 76]. In this context it is worth mentioning that during the experiments conducted for the present study different types of carbon are of relevance. Figure 7 shows the different types of carbon as found at several sampling points in the setup, irrespective of the feed gas composition. On the bottom flange, a fine, homogeneous solid carbon film deposits (Fig. 7a), which mainly consists of very fine-grained, black, adhering soot particles that predominantly form during gas-phase pyrolysis reactions as reported in some of our previous studies [32, 78]. In addition, light gray shiny carbon with a rather graphitic structure deposits on the inner reactor wall in the hot zone (Fig. 7b) that has been observed in the past as well [40]. Notably, similar gray deposits are found on the acetylene coke used as carbon particles bed, which points to an ordered carbon structure (Fig. 7c and d). Herein, the formation of  $C_2$  hydrocarbons, benzene, and condensed-phase PAH results in soot production first. Subsequently, the formed incipient soot particles further grow by both coagulation and gas-to-particle conversion until ultimately graphitic structures are formed by a further loss of hydrogen during the high-temperature pyrolysis process [79, 80].

**Fig. 6** Empty tube and fixed bed results for solid carbon yield for pure  $CH_4$  and SNG as a function of temperature and  $H_2$  dilution ratio at a constant residence time of 5 s



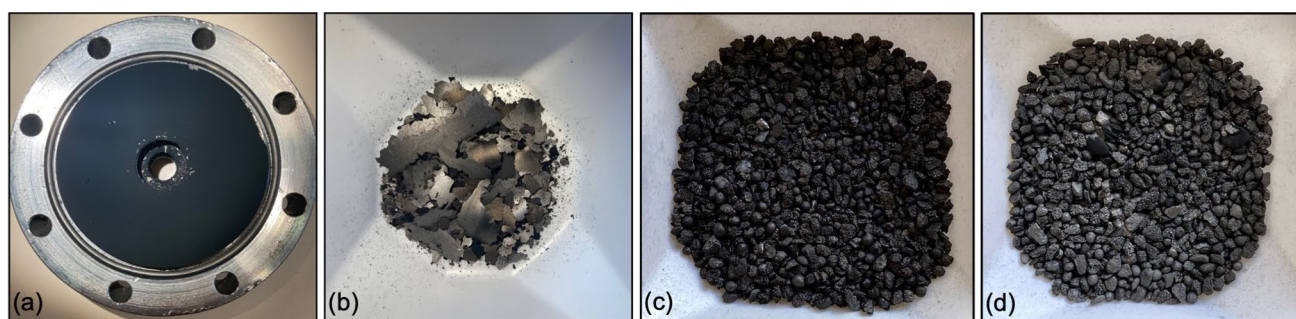


**Fig. 7** Coke formation after a fixed-bed reaction with pure  $\text{CH}_4$  at  $1400^\circ\text{C}$ , molar  $\text{H}_2$  dilution ratio of 1:1 and a residence time of 5 s. **a** Carbon deposits accumulating on the lower setup flange, **b** carbon that deposits on the walls of the reactor tube, **c** acetylene coke before the reaction, and **d** acetylene coke after the reaction

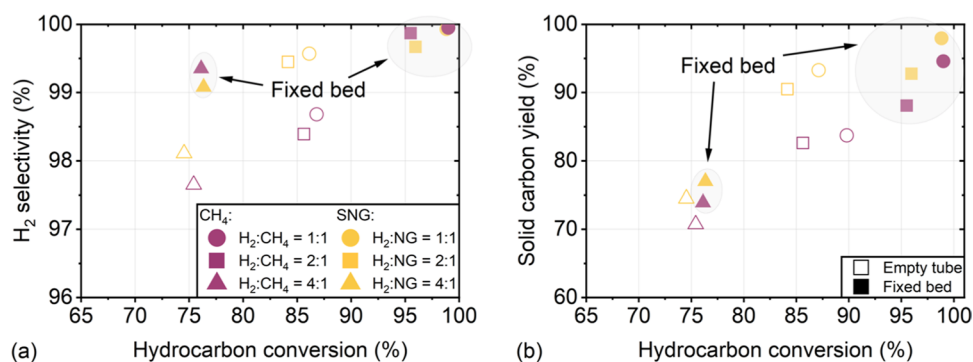
A detailed analysis of the accruing carbon is beyond the scope of our present study. However, future studies that correlate the feed gas composition with the solid product are highly desirable, because the different carbon structures and morphologies that may form during the pyrolysis process can be commercialized in different ways. For instance, acetylene coke or carbon black can be used as a pigment for the tire industry, whereas graphitic carbon can be used for electrodes [80–82]. Consequently, this also has a strong influence on the sales price. For instance, carbon in the form of coke can be sold for 150–400 \$/t, carbon black for over 1000 \$/t, activated carbon for 2000 \$/t, graphite for over 10,000 \$/t, and carbon filaments can achieve prices that exceed 1 million \$/t [81] (all prices given in US Dollar). Even if our results do not yet allow a conclusive assessment of the extent to which and what type of commercial carbon can be produced by the pyrolysis process, the amount of (partially graphitized) soot particles and acetylene coke particles after the reaction indicates that coke and carbon black are realistic assumptions for solid products. Theoretically, graphite or diamonds are also possible as target products and both have already been discussed in the literature [83, 84], but the respective processes enabling their formation are not technically mature yet. On the contrary, marketing the carbon as coke or carbon black in the price range below 1000 \$/t could already be sufficient for a profitable operation of the pyrolysis process (compared to steam reforming and electrolysis) [85], which makes the findings of the current study encouraging.

As demonstrated in the present study, the non-methane hydrocarbons and  $\text{N}_2$  in natural gas can change the reaction network, which may also impact the carbon properties to some extent. Equally important, sustainable biogas contains large amounts of  $\text{CO}_2$  that allows for a variety of additional reactions such as reverse water gas shift or dry reforming [58], and its use may result in an incorporation of oxygen into the captured carbon. This is of particular importance since depending on the area of application the solid material needs to exhibit a certain degree of purity. From mechanistic studies it is well known that the formation of solid carbon species at the interface of homogeneous and heterogeneous chemistry involves PAHs with a high boiling temperature, which are present in the liquid state at standard conditions [32, 64, 86]. As the reactor bottom where soot particles deposit (Fig. 7a) is comparably cold, we can speculate that PAHs—if at all—predominantly condensate on these soot particles, whereas the carbon in the hot zone is mostly free of PAH impurities. Therefore, soot particles and PAH are mainly formed downstream the bed or in an empty reactor. Particularly PAH formation can be minimized or even avoided either by applying higher temperatures downstream and quenching afterwards or by filling up the entire reactor with carbon particles. One of our future studies will focus on such aspects in more detail.

Since the data shown in the present study are collected during experimental runs that last 20 min, the advantageous faster deposition of non-methane hydrocarbons accelerates over time because it promotes an autocatalytic pyrolysis reaction. Analogous to findings on gas-phase  $\text{CH}_4$  pyrolysis [40], this autocatalytic process causes relevant improvements in the carbon yield and  $\text{H}_2$  selectivity, as also underscored by the data shown in Fig. 8 that summarize the results on hydrogen production and carbon capture during pyrolysis experiments in an empty tube and fixed bed reactor configuration as obtained under the conditions applied in our present study.

The data depicted in Fig. 8a illustrate that the use of a carbonaceous fixed bed increases both  $\text{CH}_4$  conversion and  $\text{H}_2$  selectivity, regardless of the used feed gas and  $\text{H}_2$  dilution. The use of SNG feeds instead of  $\text{CH}_4$ -only feeds results in slightly higher  $\text{H}_2$  selectivities under the same reaction conditions. Figure 8b underscores that the use of a fixed bed also benefits the yield of solid carbon and thus the carbon capture efficiency of the pyrolysis process for both feed gas streams. If SNG is used as feed, solid carbon yields of almost 100% can be achieved, which corresponds to a  $\text{CH}_4$

**Fig. 8** Empty tube and fixed bed results for H<sub>2</sub> selectivity (a) and solid carbon yield (b) as a function of CH<sub>4</sub> conversion and H<sub>2</sub> dilution for both, pure CH<sub>4</sub> and SNG, at a constant temperature of 1400 °C and a residence time of 5 s. Full symbols: fixed bed experiments. Edge symbols: empty tube experiments



conversion of over 98%. This clearly underlines the flexibility of the pyrolysis process with respect to the feed gas as well as its potential to act as a carbon sink.

## 4 Conclusions and outlook

Our work evaluates the usage of pure CH<sub>4</sub> and conventional natural gas under thermal pyrolysis conditions with respect to the influence of temperature, residence time, and H<sub>2</sub> dilution ratio on product composition, CH<sub>4</sub> conversion, H<sub>2</sub> selectivity, and carbon capture. For both feed gas streams used herein, namely pure CH<sub>4</sub> and SNG, hydrocarbon conversions higher than 80% and H<sub>2</sub> selectivities higher than 90% are achieved at temperatures above 1400 °C. With higher residence time, hydrocarbon conversion and H<sub>2</sub> selectivity increase significantly, which is particularly relevant at lower temperatures and becomes less relevant once temperatures of 1400 °C or more are chosen. Similarly, the inhibition effect of H<sub>2</sub> dilution on CH<sub>4</sub> conversion and H<sub>2</sub> selectivity decreases at 1400 °C and above. By a simple gas-phase pyrolysis process under optimal conditions (temperature of 1400 °C, a H<sub>2</sub> dilution of 1:1, and a residence time of 7 s), more than 90% of carbon entering the reactor are captured in the form of solid carbon.

Although somewhat lower hydrocarbon conversions are achieved during experiments with an SNG feed, most likely due to a higher effective H<sub>2</sub> dilution ratio, higher H<sub>2</sub> selectivities are observed than during experiments with CH<sub>4</sub>-only feed gas streams. We attribute this to the additional non-methane hydrocarbons that are present in the SNG feed gas stream, which represent intermediates within the CH<sub>4</sub> pyrolysis reaction network. The decomposition of these non-methane hydrocarbons leads to the formation of methyl radicals, thus generally accelerating dehydrogenation steps and increasing the relative amount of H<sub>2</sub> formed from CH<sub>4</sub>. Ultimately, this can lead to an increase in H<sub>2</sub> selectivity of almost 5%. Introducing a carbonaceous fixed bed into the reactor seems to promote the positive effect of non-methane hydrocarbons on the overall performance of the pyrolysis process and enables increased hydrocarbon conversions, H<sub>2</sub> selectivities, and solid carbon yields of over 98% at a temperature of 1400 °C, a residence time of 5 s, and a H<sub>2</sub> dilution ratio of 1:1.

Beyond CH<sub>4</sub> conversion and H<sub>2</sub> selectivity, the product gas composition data obtained herein imply several aspects that are of importance for a technical realization of the pyrolysis process. While CH<sub>4</sub>-only feeds result in hydrocarbons as only relevant byproducts, the use of natural gas would additionally require the separation of N<sub>2</sub>, CO, and CO<sub>2</sub>. Since the results indicate that comparable CH<sub>4</sub> conversions and particularly higher H<sub>2</sub> selectivities can be achieved when SNG is used instead of a CH<sub>4</sub>-only feed, an upstream purification of natural gas to remove hydrocarbons such as ethane, propane or butane might not be mandatory. Since N<sub>2</sub> as well as CO<sub>2</sub> were found to be of minor relevance with respect to their direct impact on the pyrolysis kinetics, their separation can be done either upstream or downstream.

In terms of economic and ecologic viability it must be taken into account that the purchase price for natural gas is currently and most likely also in the foreseeable future lower than the price for pure CH<sub>4</sub>, e.g. from climate-friendly power-to-gas processes [87]. Thus, there is a trade-off between costs for the feedstock and costs for additional downstream purification. In this respect, natural gas can serve as a transitional solution until sufficient amounts of renewable CH<sub>4</sub> from power-to-gas or fermentation of biomass are produced. Hence, on the way towards commercialization of the pyrolysis process, a techno-economic case study of the overall process should consider different feed compositions, such as pure CH<sub>4</sub>, natural gas, and potentially sustainable biogas that can be obtained from fermentation of biomass. If such economic aspects are considered along with technical aspects as discussed in our present study, the optimization



of process parameters will finally enable an economically attractive and climate-friendly production of hydrogen and simultaneous carbon capture by thermal pyrolysis.

**Acknowledgements** We thank M. Bender, J. Bode, K. Ehrhardt, D. Flick, F. Scheiff, and D. Schlereth (BASF) as well as M. Mokashi and A. B. Shirsath (ITCP, KIT) for fruitful discussions, M. Berg and C. Kroll (Berg-idl GmbH) for their support in engineering the high-temperature vessel of the experimental setup, and S. Lichtenberg (ITCP, KIT) for technical support during the experimental measurement campaign.

**Author contributions** AÇ: Writing – original draft, Visualization, Validation, Methodology, Investigation, Formal analysis, Data curation, Conceptualization. IBO: Investigation, Formal analysis, Writing – review & editing. HM: Investigation, Formal analysis, Writing – review & editing. OD: Conceptualization, Supervision, Resources, Project administration, Resources, Writing – review & editing. PL: Writing – original draft, Supervision, Project administration, Data curation, Conceptualization, Resources.

**Funding** Not applicable.

**Data availability** Data is provided within the manuscript. Raw data will be provided by the corresponding author upon request.

**Code availability** Not applicable.

## Declarations

**Competing interests** The authors declare no competing interests.

**Open Access** This article is licensed under a Creative Commons Attribution-NonCommercial-NoDerivatives 4.0 International License, which permits any non-commercial use, sharing, distribution and reproduction in any medium or format, as long as you give appropriate credit to the original author(s) and the source, provide a link to the Creative Commons licence, and indicate if you modified the licensed material. You do not have permission under this licence to share adapted material derived from this article or parts of it. The images or other third party material in this article are included in the article's Creative Commons licence, unless indicated otherwise in a credit line to the material. If material is not included in the article's Creative Commons licence and your intended use is not permitted by statutory regulation or exceeds the permitted use, you will need to obtain permission directly from the copyright holder. To view a copy of this licence, visit <http://creativecommons.org/licenses/by-nc-nd/4.0/>.

## References

1. Muradov N, Veziroğlu T. From hydrocarbon to hydrogen–carbon to hydrogen economy. *Int J Hydrog Energy*. 2005;30:225–37. <https://doi.org/10.1016/j.ijhydene.2004.03.033>.
2. Machhammer O, Bode A, Hormuth W. Financial and ecological evaluation of hydrogen production processes on large scale. *Chem Eng Technol*. 2016;39:1185–93. <https://doi.org/10.1002/ceat.201600023>.
3. Lott P, Deutschmann O. Heterogeneous chemical reactions—a cornerstone in emission reduction of local pollutants and greenhouse gases. *Proc Combust Inst*. 2023;39:3183–215. <https://doi.org/10.1016/j.proci.2022.06.001>.
4. Lott P, Wagner U, Koch T, Deutschmann O. Hydrogen combustion engines - chances and challenges on the way towards a decarbonized mobility. *Chem Ing Tech*. 2022;94:217–29. <https://doi.org/10.1002/cite.202100155>.
5. Sun Z, Hong J, Zhang T, Sun B, Yang B, Lu L, Li L, Wu K. Hydrogen engine operation strategies: recent progress, industrialization challenges, and perspectives. *Int J Hydrog Energy*. 2023;48:366–92. <https://doi.org/10.1016/j.ijhydene.2022.09.256>.
6. Aminudin MA, Kamarudin SK, Lim BH, Majilan EH, Masdar MS, Shaari N. An overview: current progress on hydrogen fuel cell vehicles. *Int J Hydrog Energy*. 2023;48:4371–88. <https://doi.org/10.1016/j.ijhydene.2022.10.156>.
7. Hwang J, Maharjan K, Cho H. A review of hydrogen utilization in power generation and transportation sectors: achievements and future challenges. *Int J Hydrog Energy*. 2023;48:28629–48. <https://doi.org/10.1016/j.ijhydene.2023.04.024>.
8. Otto A, Robinius M, Grube T, Schiebahn S, Praktiknjo A, Stolten D. Power-to-steel: reducing CO<sub>2</sub> through the integration of renewable energy and hydrogen into the german steel industry. *Energies*. 2017;10:451. <https://doi.org/10.3390/en10040451>.
9. Tang J, Chu MS, Li F, Feng C, Liu ZG, Zhou YS. Development and progress on hydrogen metallurgy. *Int J Miner Metall Mater*. 2020;27:713–23. <https://doi.org/10.1007/s12613-020-2021-4>.
10. Liu W, Zuo H, Wang J, Xue Q, Ren B, Yang F. The production and application of hydrogen in steel industry. *Int J Hydrog Energy*. 2021;46:10548–69. <https://doi.org/10.1016/j.ijhydene.2020.12.123>.
11. Younas M, Shafique S, Hafeez A, Javed F, Rehman F. An overview of hydrogen production: current status, potential, and challenges. *Fuel*. 2022;316: 123317. <https://doi.org/10.1016/j.fuel.2022.123317>.
12. Rosner F, Bhagde T, Slaughter DS, Zorba V, Stokes-Draut J. Techno-economic and carbon dioxide emission assessment of carbon black production. *J Cleaner Prod*. 2024;436: 140224. <https://doi.org/10.1016/j.jclepro.2023.140224>.
13. Fulcheri L, Rohani V-J, Wyse E, Hardman N, Dames E. An energy-efficient plasma methane pyrolysis process for high yields of carbon black and hydrogen. *Int J Hydrog Energy*. 2023;48:2920–8. <https://doi.org/10.1016/j.ijhydene.2022.10.144>.
14. Patlolla SR, Katsu K, Sharafian A, Wei K, Herrera OE, Mérida W. A review of methane pyrolysis technologies for hydrogen production. *Renew Sustain Energy Rev*. 2023;181: 113323. <https://doi.org/10.1016/j.rser.2023.113323>.



15. Bode A, Flick D. Methane pyrolysis—a potential new process for hydrogen production without CO<sub>2</sub> emission. <https://arpa-e.energy.gov/sites/default/files/2021-01/16%20OK%20-%20ARPA-E%20Meeting%20Bode%20Flick%20Methane%20Pyrolysis%20web.pdf>. Accessed on 23 Aug 2024.
16. Daghighaleh O, Schenk J, Zarl MA, Lehner M, Farkas M, Zheng H. Feasibility of a plasma furnace for methane pyrolysis: hydrogen and carbon production. *Energies*. 2024;17:167. <https://doi.org/10.3390/en17010167>.
17. Sánchez-Bastardo N, Schlögl R, Ruland H. Methane pyrolysis for zero-emission hydrogen production: a potential bridge technology from fossil fuels to a renewable and sustainable hydrogen economy. *Ind Eng Chem Res*. 2021;60:11855–81. <https://doi.org/10.1021/acs.iecr.1c01679>.
18. Schneider S, Bajohr S, Graf F, Kolb T. State of the art of hydrogen production via pyrolysis of natural gas. *ChemBioEng Rev*. 2020;7:150–8. <https://doi.org/10.1002/cben.202000014>.
19. Christopher K, Dimitrios R. A review on exergy comparison of hydrogen production methods from renewable energy sources. *Energy Environ Sci*. 2012;5:6640–51. <https://doi.org/10.1039/c2ee01098d>.
20. Hermesmann M, Müller TE. Green, turquoise, blue, or grey? Environmentally friendly hydrogen production in transforming energy systems. *Prog Energy Combust Sci*. 2022;90: 100996. <https://doi.org/10.1016/j.pecs.2022.100996>.
21. Muradov N. Low to near-zero CO<sub>2</sub> production of hydrogen from fossil fuels: status and perspectives. *Int J Hydrog Energy*. 2017;42:14058–88. <https://doi.org/10.1016/j.ijhydene.2017.04.101>.
22. Parkinson B, Balcombe P, Speirs JF, Hawkes AD, Hellgardt K. Levelized cost of CO<sub>2</sub> mitigation from hydrogen production routes. *Energy Environ Sci*. 2019;12:19–40. <https://doi.org/10.1039/c8ee02079e>.
23. Parkinson B, Tabatabaei M, Upham DC, Ballinger B, Greig C, Smart S, McFarland E. Hydrogen production using methane: techno-economics of decarbonizing fuels and chemicals. *Int J Hydrog Energy*. 2018;43:2540–55. <https://doi.org/10.1016/j.ijhydene.2017.12.081>.
24. Abbas HF, Wan Daud WMA. Hydrogen production by methane decomposition: a review. *Int J Hydrog Energy*. 2010;35:1160–90. <https://doi.org/10.1016/j.ijhydene.2009.11.036>.
25. Ashik UPM, Wan Daud WMA, Abbas HF. Production of greenhouse gas free hydrogen by thermocatalytic decomposition of methane—a review. *Renew Sustain Energy Rev*. 2015;44:221–56. <https://doi.org/10.1016/j.rser.2014.12.025>.
26. Olsvik O, Rokstad OA, Holmen A. Pyrolysis of methane in the presence of hydrogen. *Chem Eng Technol*. 1995;18:349–58. <https://doi.org/10.1002/ceat.270180510>.
27. National Institute of Standards and Technology (NIST). NIST Chemistry WebBook, SRD69. <https://webbook.nist.gov/chemistry/>. Accessed on 8 Oct 2024.
28. Chen C-J, Back MH, Back RA. Mechanism of the thermal decomposition of methane. In: Albright LF, Crynes BL, editors. *Industrial and laboratory pyrolyses*. Washington, D.C: American Chemical Society; 1976. p. 1–16. <https://doi.org/10.1021/bk-1976-0032.ch001>.
29. Holmen A, Olsvik O, Rokstad OA. Pyrolysis of natural gas: chemistry and process concepts. *Fuel Process Technol*. 1995;42:249–67. [https://doi.org/10.1016/0378-3820\(94\)00109-7](https://doi.org/10.1016/0378-3820(94)00109-7).
30. Benzinger W, Becker A, Hüttinger KJ. Chemistry and kinetics of chemical vapour deposition of pyrocarbon: I. Fundamentals of kinetics and chemical reaction engineering. *Carbon*. 1996;34:957–66. [https://doi.org/10.1016/0008-6223\(96\)00010-3](https://doi.org/10.1016/0008-6223(96)00010-3).
31. Appel J, Bockhorn H, Frenklach M. Kinetic modeling of soot formation with detailed chemistry and physics: laminar premixed flames of C<sub>2</sub> hydrocarbons. *Combust Flame*. 2000;121:122–36. [https://doi.org/10.1016/s0010-2180\(99\)00135-2](https://doi.org/10.1016/s0010-2180(99)00135-2).
32. Shirsath AB, Mokashi M, Lott P, Müller H, Pashminehazar R, Sheppard T, Tischer S, Maier L, Grunwaldt J-D, Deutschmann O. Soot formation in methane pyrolysis reactor: modeling soot growth and particle characterization. *J Phys Chem A*. 2023;127:2136–47. <https://doi.org/10.1021/acs.jpca.2c06878>.
33. Norinaga K, Deutschmann O, Saegusa N, Hayashi J-I. Analysis of pyrolysis products from light hydrocarbons and kinetic modeling for growth of polycyclic aromatic hydrocarbons with detailed chemistry. *J Anal Appl Pyrolysis*. 2009;86:148–60. <https://doi.org/10.1016/j.jaap.2009.05.001>.
34. Norinaga K, Deutschmann O. Detailed kinetic modeling of gas-phase reactions in the chemical vapor deposition of carbon from light hydrocarbons. *Ind Eng Chem Res*. 2007;46:3547–57. <https://doi.org/10.1021/ie061207p>.
35. Abánades A, Ruiz E, Ferruelo EM, Hernández F, Cabanillas A, Martínez-Val JM, Rubio JA, López C, Gavela R, Barrera G, Rubbia C, Salmieri D, Rodilla E, Gutiérrez D. Experimental analysis of direct thermal methane cracking. *Int J Hydrog Energy*. 2011;36:12877–86. <https://doi.org/10.1016/j.ijhydene.2011.07.081>.
36. Zhou L, Enakonda LR, Harb M, Saih Y, Aguilar-Tapia A, Ould-Chikh S, Hazemann J-L, Li J, Wei N, Gary D, Del-Gallo P, Basset J. Fe catalysts for methane decomposition to produce hydrogen and carbon nano materials. *Appl Catal B*. 2017;208:44–59. <https://doi.org/10.1016/j.fuel.2013.02.016>.
37. Sharif Zein SH, Mohamed AR, Talpa Sai PS. Kinetic studies on catalytic decomposition of methane to hydrogen and carbon over Ni/TiO<sub>2</sub> catalyst. *Ind Eng Chem Res*. 2004;43:4864–70. <https://doi.org/10.1021/ie034208f>.
38. Korányi TI, Németh M, Beck A, Horváth A. Recent advances in methane pyrolysis: turquoise hydrogen with solid carbon production. *Energies*. 2022. <https://doi.org/10.3390/en15176342>.
39. Timmerberg S, Kaltschmitt M, Finkbeiner M. Hydrogen and hydrogen-derived fuels through methane decomposition of natural gas—GHG emissions and costs. *Energy Convers Manage X*. 2020;7: 100043. <https://doi.org/10.1016/j.ecmx.2020.100043>.
40. Lott P, Mokashi MB, Müller H, Heitlinger DJ, Lichtenberg S, Shirsath AB, Janzer C, Tischer S, Maier L, Deutschmann O. Hydrogen production and carbon capture by gas phase methane pyrolysis: a feasibility study. *ChemSusChem*. 2023;16:e202201720. <https://doi.org/10.1002/cssc.202201720>.
41. Serrano DP, Botas J, Pizarro P, Gómez-Pozuelo G. Kinetic and autocatalytic effects during the hydrogen production by methane decomposition over carbonaceous catalysts. *Int J Hydrogen Energy*. 2013;38:5671–83. <https://doi.org/10.1016/j.ijhydene.2013.02.112>.
42. Serrano DP, Botas JA, Fierro JLG, Guil-López R, Pizarro P, Gómez G. Hydrogen production by methane decomposition: origin of the catalytic activity of carbon materials. *Fuel*. 2010;89:1241–8. <https://doi.org/10.1016/j.fuel.2009.11.030>.
43. Zhang J, Li X, Chen H, Qi M, Zhang G, Hu H, Ma X. Hydrogen production by catalytic methane decomposition: carbon materials as catalysts or catalyst supports. *Int J Hydrog Energy*. 2017;42:19755–75. <https://doi.org/10.1016/j.ijhydene.2017.06.197>.

44. Ong SH, Tan RR, Andiappan V. Optimisation of biochar-based supply chains for negative emissions and resource savings in carbon management networks. *Clean Technol Environ Policy*. 2021;23:621–38. <https://doi.org/10.1007/s10098-020-01990-0>.
45. Zhang F, Ma C, Huang X, Liu J, Lu L, Peng K, Li S. Research progress in solid carbon source-based denitrification technologies for different target water bodies. *Sci Total Environ*. 2021;782: 146669. <https://doi.org/10.1016/j.scitotenv.2021.146669>.
46. Carbon black market analysis. <https://www.chemanalyst.com/industry-report/carbon-black-market-440>. Accessed on 2 Aug 2024.
47. Rasul MG, Hazrat MA, Sattar MA, Jahirul MI, Shearer MJ. The future of hydrogen: challenges on production, storage and applications. *Energy Convers Manage*. 2022;272: 116326. <https://doi.org/10.1016/j.enconman.2022.116326>.
48. Ukwattage NL, Ranjith PG, Bouazza M. The use of coal combustion fly ash as a soil amendment in agricultural lands (with comments on its potential to improve food security and sequester carbon). *Fuel*. 2013;109:400–8. <https://doi.org/10.1016/j.fuel.2013.02.016>.
49. Faramawy S, Zaki T, Sakr AA. Natural gas origin, composition, and processing: a review. *J Nat Gas Sci Eng*. 2016;34:34–54. <https://doi.org/10.1016/j.jngse.2016.06.030>.
50. Ahmed S, Aitani A, Rahman F, Al-Dawood A, Al-Muhaish F. Decomposition of hydrocarbons to hydrogen and carbon. *Appl Catal A*. 2009;359:1–24. <https://doi.org/10.1016/j.apcata.2009.02.038>.
51. Gaudernack B, Lynum S. Hydrogen from natural gas without release of CO<sub>2</sub> to the atmosphere. *Int J Hydrog Energy*. 1998;23:1087–93. [https://doi.org/10.1016/S0360-3199\(98\)00004-4](https://doi.org/10.1016/S0360-3199(98)00004-4).
52. Muradov N. Emission-free fuel reformers for mobile and portable fuel cell applications. *J Power Sources*. 2003;118:320–4. [https://doi.org/10.1016/S0378-7753\(03\)00078-8](https://doi.org/10.1016/S0378-7753(03)00078-8).
53. Serban M, Lewis MA, Marshall CL, Doctor RD. Hydrogen production by direct contact pyrolysis of natural gas. *Energy Fuels*. 2003;17:705–13. <https://doi.org/10.1021/ef020271q>.
54. Mašláni A, Hlína M, Hrabovský M, Křenek P, Sikarwar VS, Fathi J, Raman S, Skoblia S, Jankovský O, Jiříčková A, Sharma S, Mates T, Mušálek R, Lukáč F, Jeremiáš M. Impact of natural gas composition on steam thermal plasma assisted pyrolysis for hydrogen and solid carbon production. *Energy Convers Manage*. 2023;297: 117748. <https://doi.org/10.1016/j.enconman.2023.117748>.
55. Wang S, Lee WJ, Ce Li, Kuan B, Burke N, Patel J. Pyrolysis of natural gas: effects of process variables and reactor materials on the product gas composition. *Chem Eng Technol*. 2019;42:690–8. <https://doi.org/10.1002/ceat.201800267>.
56. Rokstad OA, Olsvik O, Holmen A. Thermal coupling of methane. In: Holmen A, Jens KJ, Kolboe S, editors. *Studies in surface science and catalysis*. Amsterdam: Elsevier; 1991. p. 533–9. [https://doi.org/10.1016/S0167-2991\(08\)60120-2](https://doi.org/10.1016/S0167-2991(08)60120-2).
57. Walter V, Göransson L, Taljegard M, Öberg S, Odenberger M. Low-cost hydrogen in the future European electricity system—enabled by flexibility in time and space. *Appl Energy*. 2023;330: 120315. <https://doi.org/10.1016/j.apenergy.2022.120315>.
58. Çelik A, Ben Othman I, Müller H, Lott P, Deutschmann O. Pyrolysis of biogas for carbon capture and carbon dioxide-free production of hydrogen. *React Chem Eng*. 2024;9:108–18. <https://doi.org/10.1039/d3re00360d>.
59. Angeli SD, Gossler S, Lichtenberg S, Kass G, Agrawal AK, Valerius M, Kinzel KP, Deutschmann O. Reduction of CO<sub>2</sub> emission from off-gases of steel industry by dry reforming of methane. *Angew Chem Int Ed*. 2021;60:11852–7. <https://doi.org/10.1002/anie.202100577>.
60. Çelik A, Shirsath AB, Sylá F, Müller H, Lott P, Deutschmann O. On the role of hydrogen inhibition in gas-phase methane pyrolysis for carbon capture and hydrogen production in a tubular flow reactor. *J Anal Appl Pyrolysis*. 2024;181: 106628. <https://doi.org/10.1016/j.jaap.2024.106628>.
61. Guéret C, Daroux M, Billaud F. Methane pyrolysis: thermodynamics. *Chem Eng Sci*. 1997;52:815–27. [https://doi.org/10.1016/S0009-2509\(96\)00444-7](https://doi.org/10.1016/S0009-2509(96)00444-7).
62. Rokstad OA, Olsvik O, Jenssen B, Holmen A. Ethylene, acetylene, and benzene from methane pyrolysis. In: Albright LF, Crynes BL, Nowak S, editors. *Novel production methods for ethylene, light hydrocarbons, and aromatics*. New York: M Dekker; 1992. p. 259–71.
63. Khan ZA, Hellier P, Ladommatos N, Almaleki A. Sampling of gas-phase intermediate pyrolytic species at various temperatures and residence times during pyrolysis of methane, ethane, and butane in a high-temperature flow reactor. *Sustainability*. 2023. <https://doi.org/10.3390/su15076183>.
64. Mokashi M, Shirsath AB, Lott P, Müller H, Tischer S, Maier L, Deutschmann O. Understanding of gas-phase methane pyrolysis towards hydrogen and solid carbon with detailed kinetic simulations and experiments. *Chem Eng J*. 2024;479: 147556. <https://doi.org/10.1016/j.cej.2023.147556>.
65. Glasier GF, Filfil R, Pacey PD. Formation of polycyclic aromatic hydrocarbons coincident with pyrolytic carbon deposition. *Carbon*. 2001;39:497–506. [https://doi.org/10.1016/S0008-6223\(00\)00156-1](https://doi.org/10.1016/S0008-6223(00)00156-1).
66. Ogiwara H, Tajima H, Kurokawa H. Pyrolysis of mixtures of methane and ethane: activation of methane with the aid of radicals generated from ethane. *React Chem Eng*. 2020;5:145–53. <https://doi.org/10.1039/c9re00400a>.
67. Billaud F, Guéret C, Weill J. Thermal decomposition of pure methane at 1263 K. Experiments and mechanistic modelling. *Thermocim Acta*. 1992;211:303–22. [https://doi.org/10.1016/0040-6031\(92\)87029-a](https://doi.org/10.1016/0040-6031(92)87029-a).
68. Hu C, Shen H, Zhang S, Li H. Methane pyrolysis in preparation of pyrolytic carbon: thermodynamic and kinetic analysis by density functional theory. *Chin J Aeronaut*. 2020;33:1064–73. <https://doi.org/10.1016/j.cja.2019.02.015>.
69. Lahijani P, Zainal ZA, Mohammadi M, Mohamed AR. Conversion of the greenhouse gas CO<sub>2</sub> to the fuel gas CO via the Boudouard reaction: a review. *Renew Sustain Energy Rev*. 2015;41:615–32. <https://doi.org/10.1016/j.rser.2014.08.034>.
70. Starkie CM, Amieiro-Fonseca A, Rigby SP, Drage TC, Lester EH. Surfactant mediated CO<sub>2</sub> adsorption; the role of the co-impregnation species. *Energy Procedia*. 2014;63:2323–30. <https://doi.org/10.1016/j.egypro.2014.11.252>.
71. Chebbi R, Qasim M, Abdel JN. Optimization of triethylene glycol dehydration of natural gas. *Energy Rep*. 2019;5:723–32. <https://doi.org/10.1016/j.egypr.2019.06.014>.
72. Luberti M, Ahn H. Review of Polybed pressure swing adsorption for hydrogen purification. *Int J Hydrog Energy*. 2022;47:10911–33. <https://doi.org/10.1016/j.ijhydene.2022.01.147>.
73. Zhu X, Shi Y, Li S, Cai N. Elevated temperature pressure swing adsorption process for reactive separation of CO/CO<sub>2</sub> in H<sub>2</sub>-rich gas. *Int J Hydrog Energy*. 2018;43:13305–17. <https://doi.org/10.1016/j.ijhydene.2018.05.030>.
74. Pinilla JL, Suelves L, Lázaro MJ, Moliner R. Influence on hydrogen production of the minor components of natural gas during its decomposition using carbonaceous catalysts. *J Power Sources*. 2009;192:100–6. <https://doi.org/10.1016/j.jpowsour.2008.12.074>.

75. Muradov N. Catalysis of methane decomposition over elemental carbon. *Catal Commun.* 2001;2:89–94. [https://doi.org/10.1016/s1566-7367\(01\)00013-9](https://doi.org/10.1016/s1566-7367(01)00013-9).
76. Muradov N, Smith F, Raissi AT. Catalytic activity of carbons for methane decomposition reaction. *Catal Today.* 2005;102:225–33. <https://doi.org/10.1016/j.cattod.2005.02.018>.
77. Serrano DP, Botas JA, Guil-Lopez R. H<sub>2</sub> production from methane pyrolysis over commercial carbon catalysts: kinetic and deactivation study. *Int J Hydrog Energy.* 2009;34:4488–94. <https://doi.org/10.1016/j.ijhydene.2008.07.079>.
78. Mokashi M, Shirsath AB, Çelik A, Lott P, Müller H, Tischler S, Maier L, Bode J, Schlereth D, Scheiff F, Flick D, Bender M, Ehrhardt K, Deutschmann O. Methane pyrolysis in packed bed reactors: kinetic modeling, numerical simulations, and experimental insights. *Chem Eng J.* 2024;485: 149684. <https://doi.org/10.1016/j.cej.2024.149684>.
79. Michelsen HA, Colket MB, Bengtsson P-E, D'Anna A, Desgroux P, Haynes BS, Miller JH, Nathan GJ, Pitsch H, Wang H. A review of terminology used to describe soot formation and evolution under combustion and pyrolytic conditions. *ACS Nano.* 2020;14:12470–90. <https://doi.org/10.1021/acs.nano.0c06226>.
80. Prabowo J, Lai L, Chivers B, Burke D, Dinh AH, Ye L, Wang Y, Wang Y, Wei L, Chen Y. Solid carbon co-products from hydrogen production by methane pyrolysis: current understandings and recent progress. *Carbon.* 2024;216: 118507. <https://doi.org/10.1016/j.carbon.2023.118507>.
81. Keipi T, Tolvanen KES, Tolvanen H, Konttinen J. Thermo-catalytic decomposition of methane: the effect of reaction parameters on process design and the utilization possibilities of the produced carbon. *Energy Convers Manage.* 2016;126:923–34. <https://doi.org/10.1016/j.enconman.2016.08.060>.
82. Ji Y, Palmer C, Foley EE, Giovine R, Yoshida E, Sebt E, Patterson AR, McFarland E, Clément RJ. Valorizing the carbon byproduct of methane pyrolysis in batteries. *Carbon.* 2023;204:26–35. <https://doi.org/10.1016/j.carbon.2022.12.044>.
83. Abuseada M, Fisher TS. Continuous solar-thermal methane pyrolysis for hydrogen and graphite production by roll-to-roll processing. *Appl Energy.* 2023;352: 121872. <https://doi.org/10.1016/j.apenergy.2023.121872>.
84. Gong Y, Luo D, Choe M, Kim Y, Ram B, Zafari M, Seong WK, Bakharev P, Wang M, Park IK, Lee S, Shin TJ, Lee Z, Lee G, Ruoff RS. Growth of diamond in liquid metal at 1 atm pressure. *Nature.* 2024;629:348–54. <https://doi.org/10.1038/s41586-024-07339-7>.
85. Keipi T, Tolvanen H, Konttinen J. Economic analysis of hydrogen production by methane thermal decomposition: comparison to competing technologies. *Energy Convers Manage.* 2018;159:264–73. <https://doi.org/10.1016/j.enconman.2017.12.063>.
86. Kholghy MR, Kelesidis GA, Pratsinis SE. Reactive polycyclic aromatic hydrocarbon dimerization drives soot nucleation. *Phys Chem Chem Phys.* 2018;20:10926–38. <https://doi.org/10.1039/c7cp07803j>.
87. Gorre J, Ortlöf F, Van Leeuwen C. Production costs for synthetic methane in 2030 and 2050 of an optimized power-to-gas plant with intermediate hydrogen storage. *Appl Energy.* 2019;253: 113594. <https://doi.org/10.1016/j.apenergy.2019.113594>.

**Publisher's Note** Springer Nature remains neutral with regard to jurisdictional claims in published maps and institutional affiliations.